Supporting Information

Efficient Photoreduction of CO_2 to CO by Co-ZIL-L Derived NiCo-OH with Ultrathin Nanosheet Assembled 2D Leaf Superstructure

Yang Zhang,[a] Wenfeng Zhong,[a] Linhai Duan,[b] Jiaping Zhu [a] and Hua Tan*, [a]

a College of Chemistry, Guangdong University of Petrochemical Technology, Maoming 525000, China

b College of Chemical Engineering, Guangdong University of Petrochemical Technology, Maoming 525000, China

Corresponding Authors: Hua Tan: huatan@gdupt.edu.cn

KEYWORDS: Metal-organic framework; photocatalysis; CO_2 reduction; nanosheet; superstructure

Photocatalytic experiments.

The apparent quantum yield (AQY) was measured by the PCX50C Discover multi-channel parallel photocatalytic reaction system (Perfect Light Co., Ltd.) with a 10 W monochromatic LED light as the light source. The number of incident photons was measured by using a radiant power energy meter (PL-MW2000 Photoradiometer, Perfect Light Co., Ltd.). The AQY was calculated according to the following equation:

$$\mathrm{AQY(CO)\%} = \frac{\text{number of reacted eletrons}}{\text{number of incident eletrons}} \times 100\%$$

$$= \frac{\text{number of evolved CO molecules} \times 2}{\text{number of incident eletrons}} \times 100\%$$

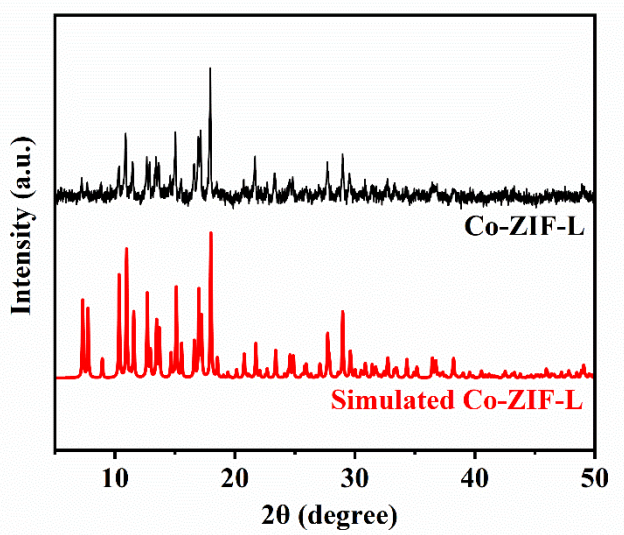

Fig. S1. XRD pattern of Co-ZIF-L.

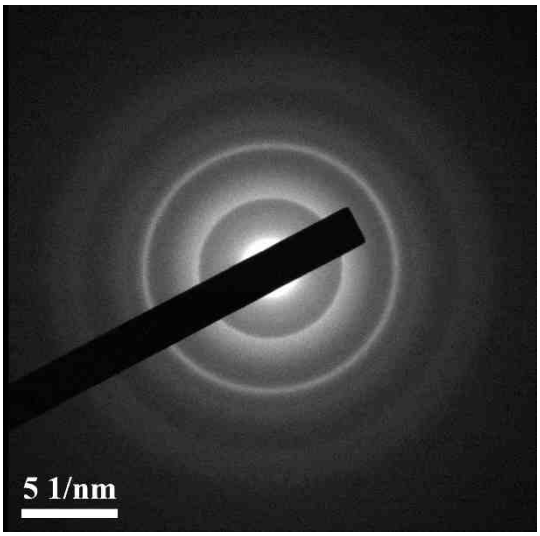

Fig. S2. The SAED pattern of NiCo-OH UNLS.

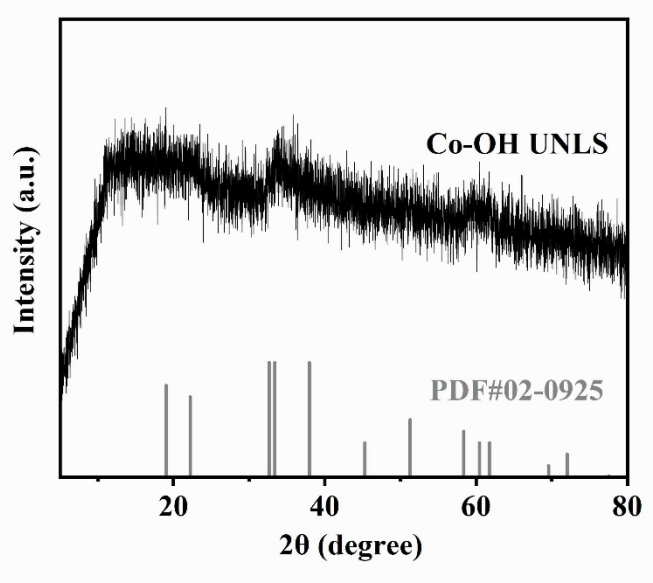

Fig. S3. XRD pattern of Co-OH UNLS.

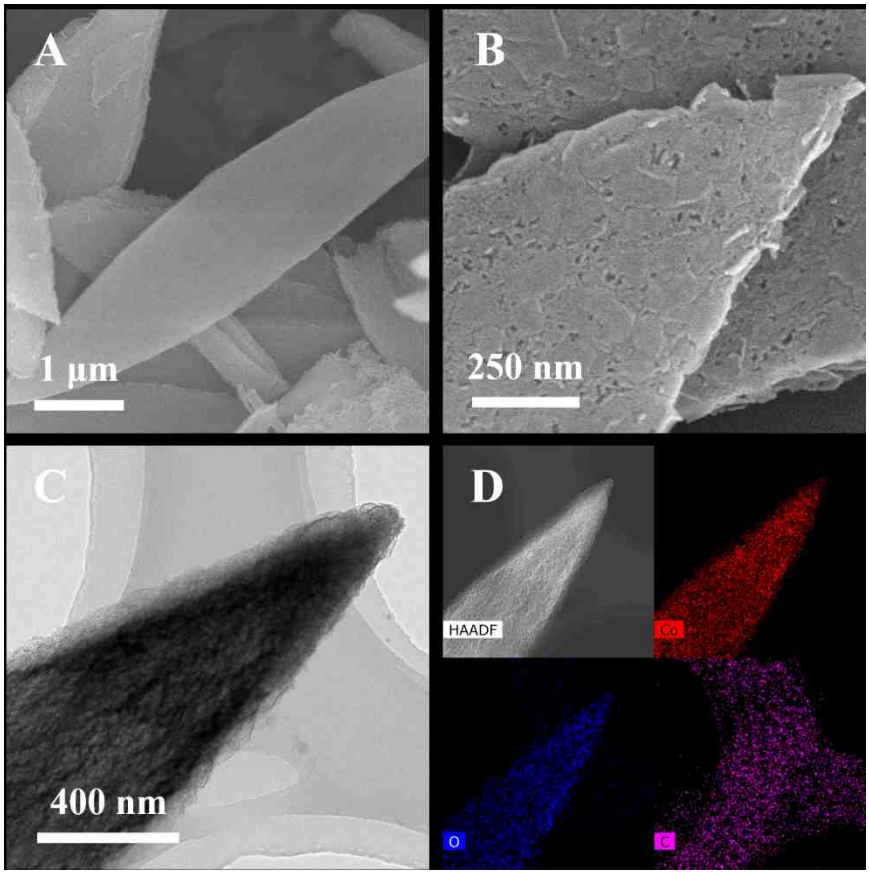

Fig. S4. (A and B) SEM images, (C) TEM image and (D) HAADF and EDX elemental mapping images of Co-OH UNLS.

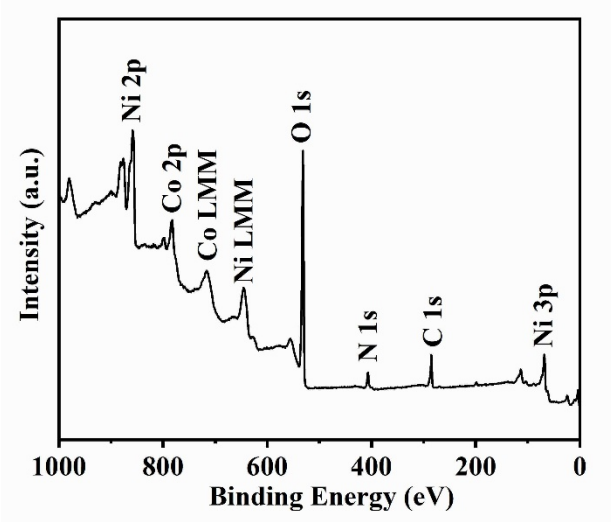

Fig. S5. XPS spectrum of NiCo-OH UNLS.

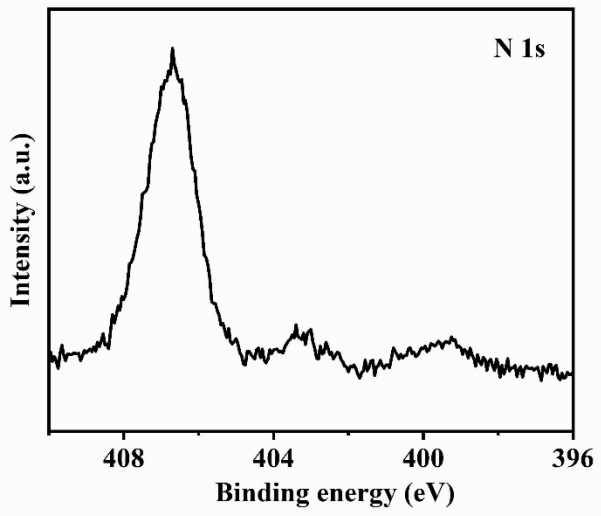

Fig. S6. High-resolution XPS spectrum of N 1s of NiCo-OH UNLS.

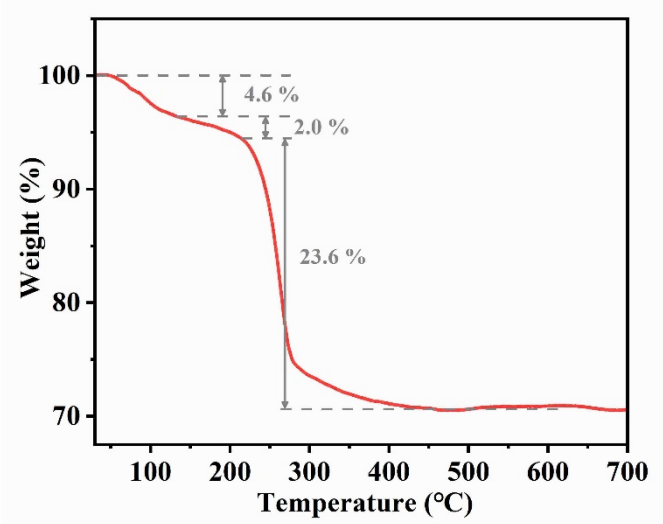

Fig. S7. TGA curves of NiCo-OH UNLS under Ar atmosphere.

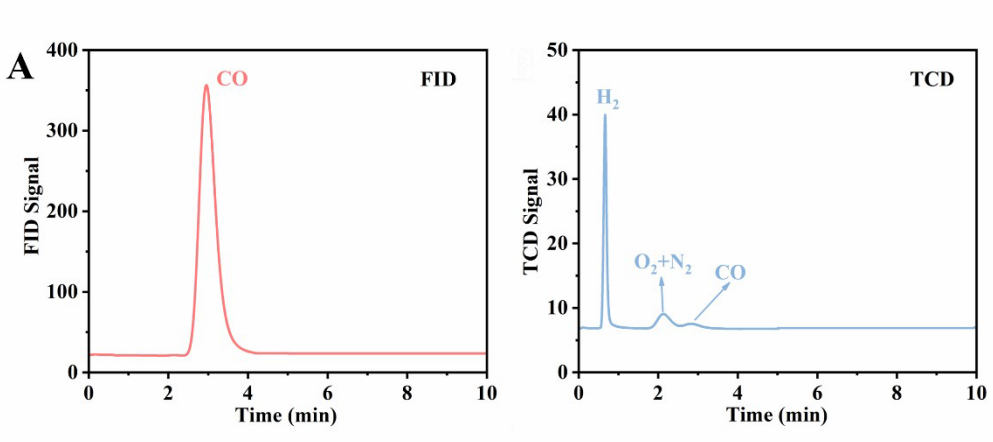

Fig. S8. (A) The FID spectrum and (B) the TCD spectrum of the gas products after reaction.

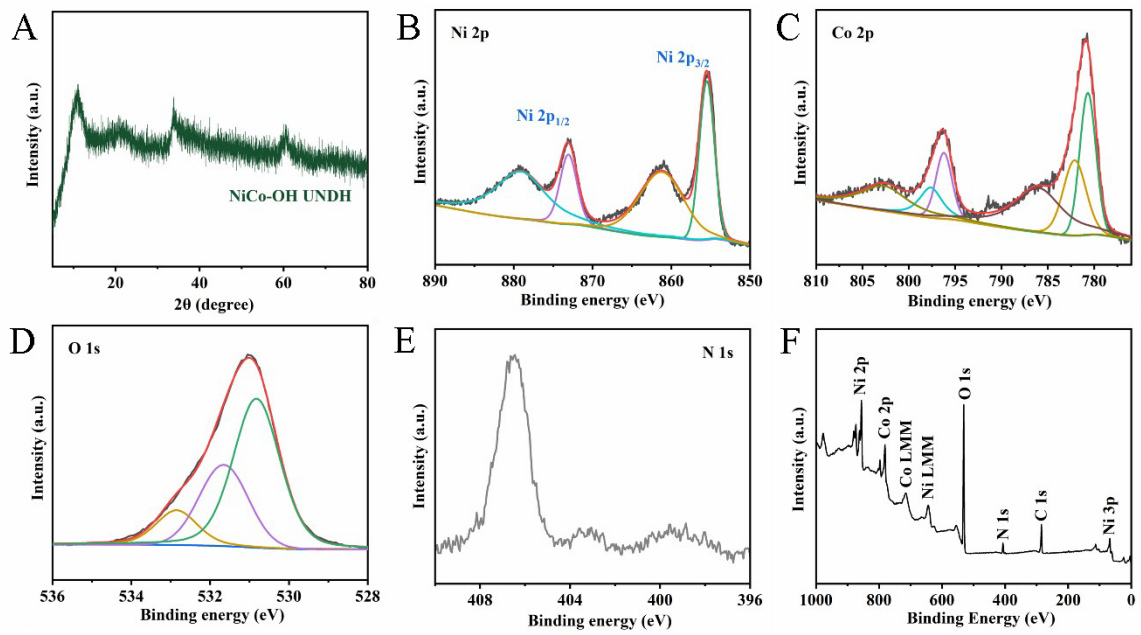

Fig. S9. (A) XRD pattern of NiCo-OH UNDH; (B) High-resolution XPS spectrum of (B) Ni 2p, (C) Co 2p, (D) O 1s and (E) O 1s of NiCo-OH UNDH; (F) XPS spectrum of NiCo-OH UNDH.

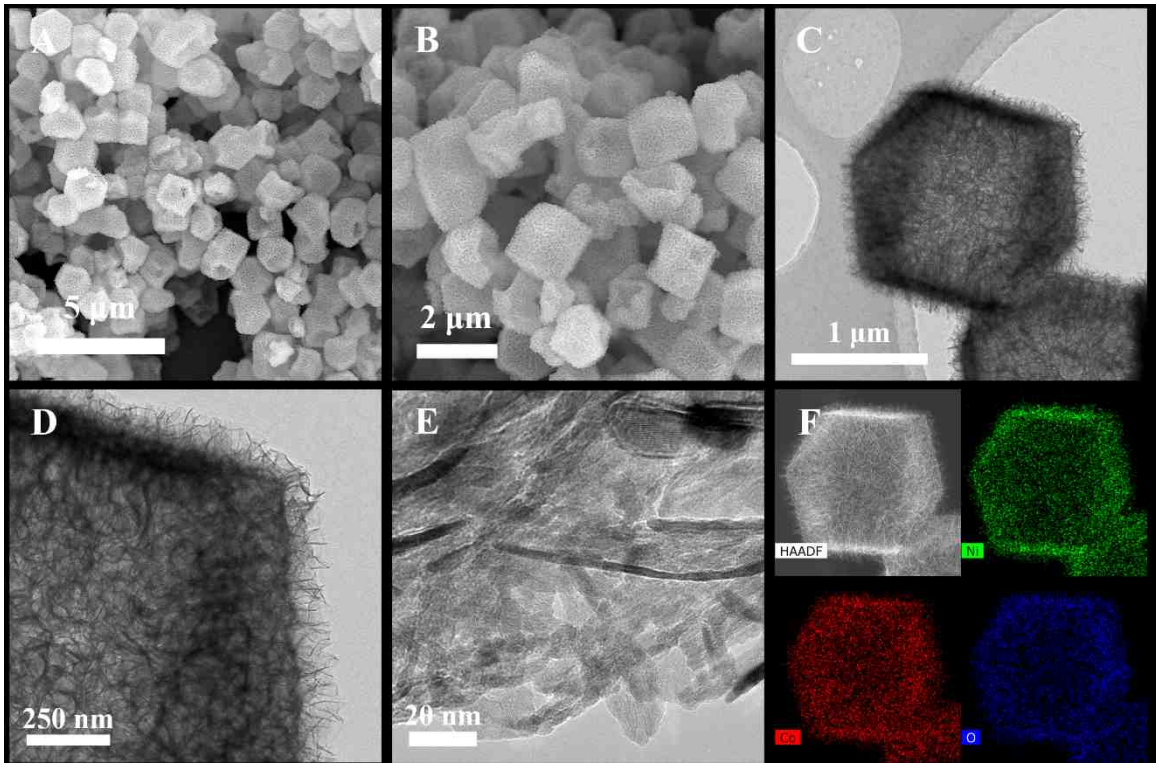

Fig. S10. (A and B) SEM, (C and D) TEM, (E) HRTEM, (F) HAADF and EDX elemental mapping images of NiCo-OH UNDH.

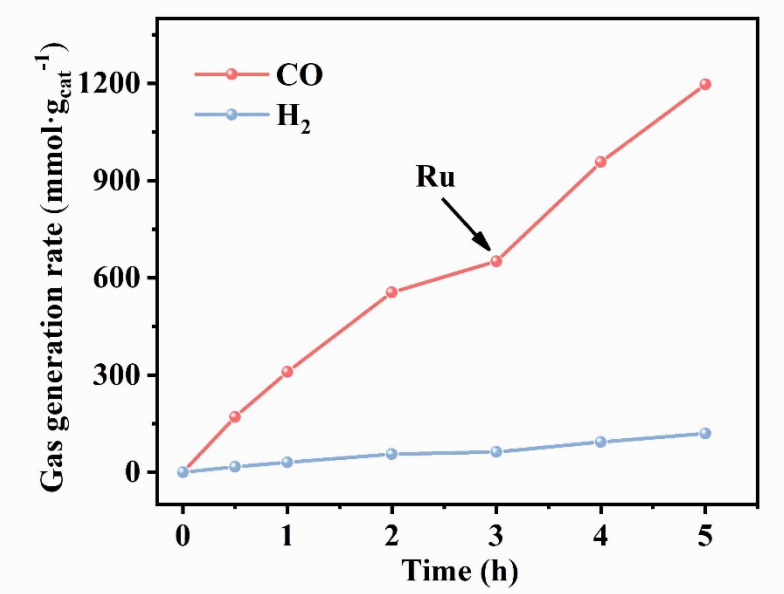

Fig. S11. Photocatalytic performance of the replenishment of photosensitizer.

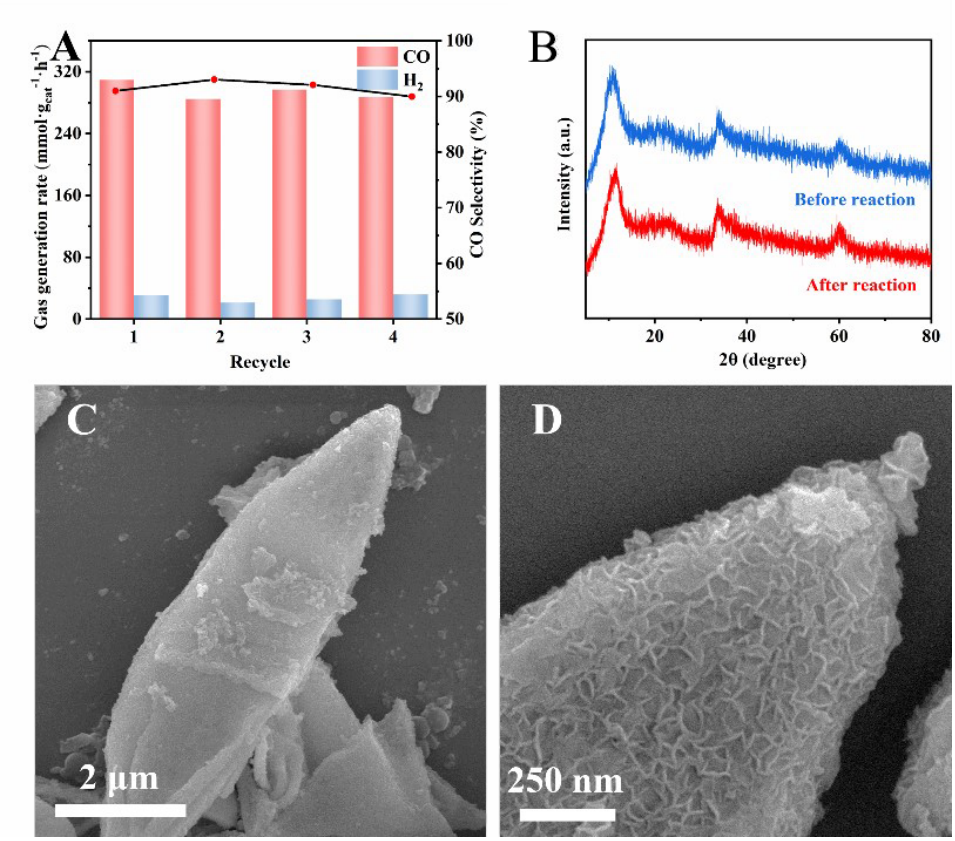

Fig. S12. (A) Multicycle photoreduction process over NiCo-OH UNLS; (B) XRD patterns of NiCo-OH UNLS before and after photocatalytic reaction; (C and D) SEM images of NiCo-OH UNLS after photocatalytic reaction.

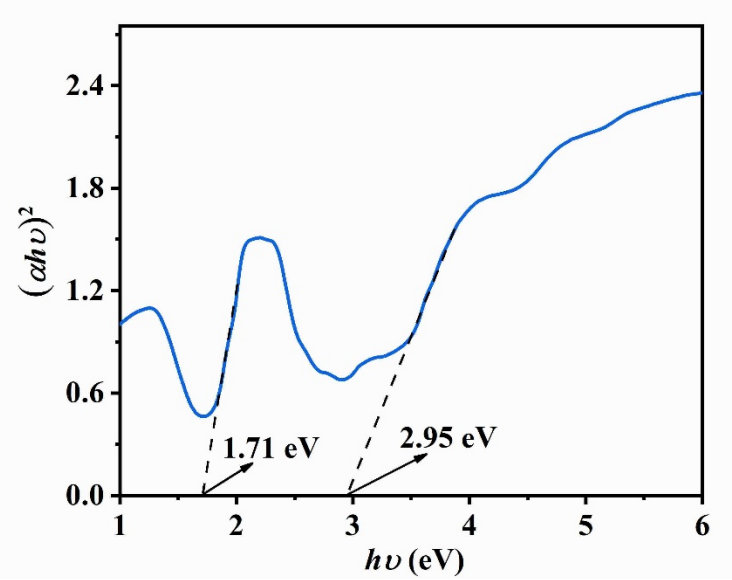

Fig. S13. Tauc plots of NiCo-OH UNLS.

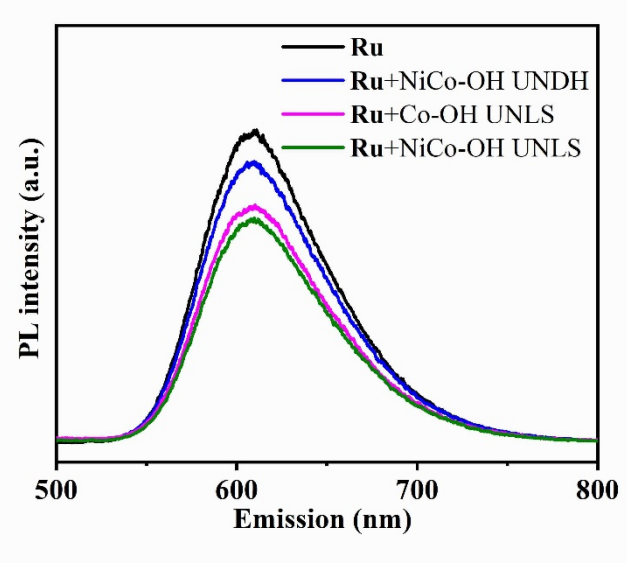

Fig. S14. Steady-state PL spectra of various catalysts.

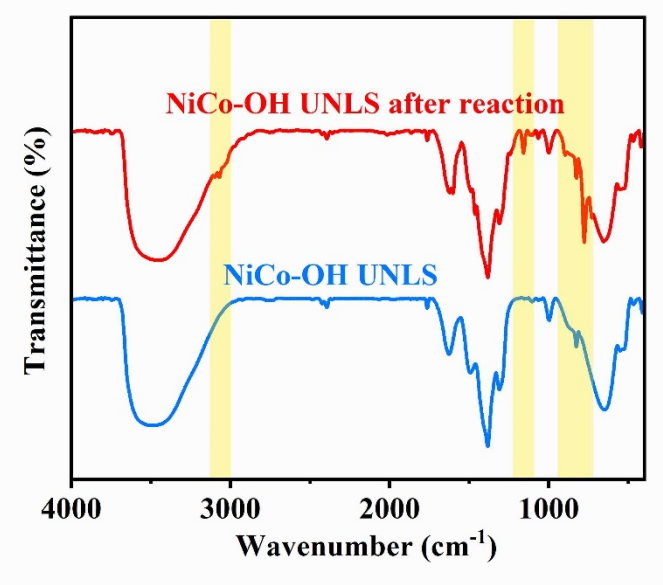

Fig. S15. FT-IR spectra of NiCo-OH UNLS before and after photocatalytic reaction.

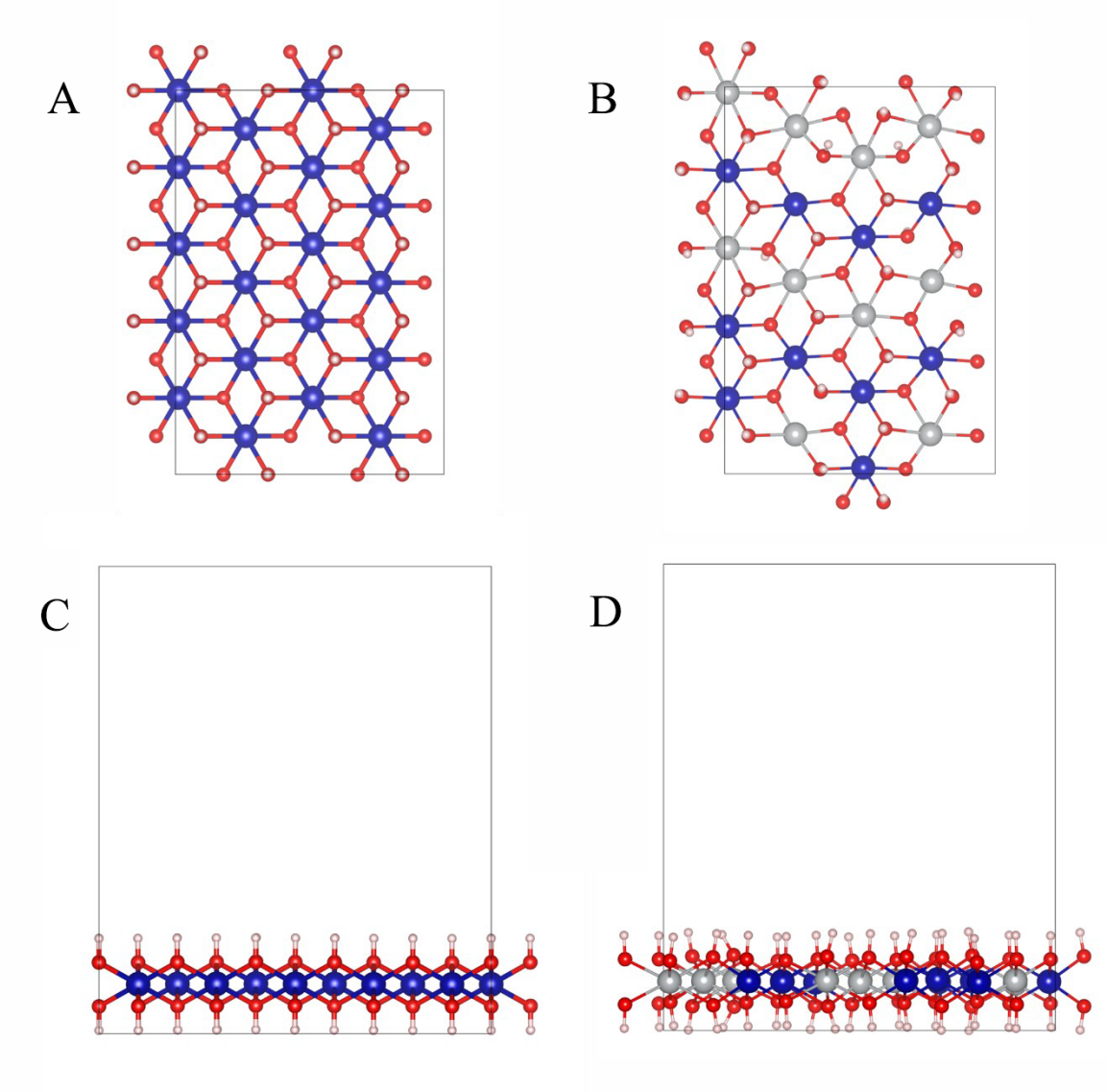

Fig. S16. The top view of optimized surface structures of (A) Co-OH UNLS and (B) Ni Co-OH UNLS models; The side view of optimized surface structures of (C) Co-OH UNLS and (D) Ni Co-OH UNLS models. Blue, gray, pink, and red balls represent Co, Ni, H and O atoms, respectively.

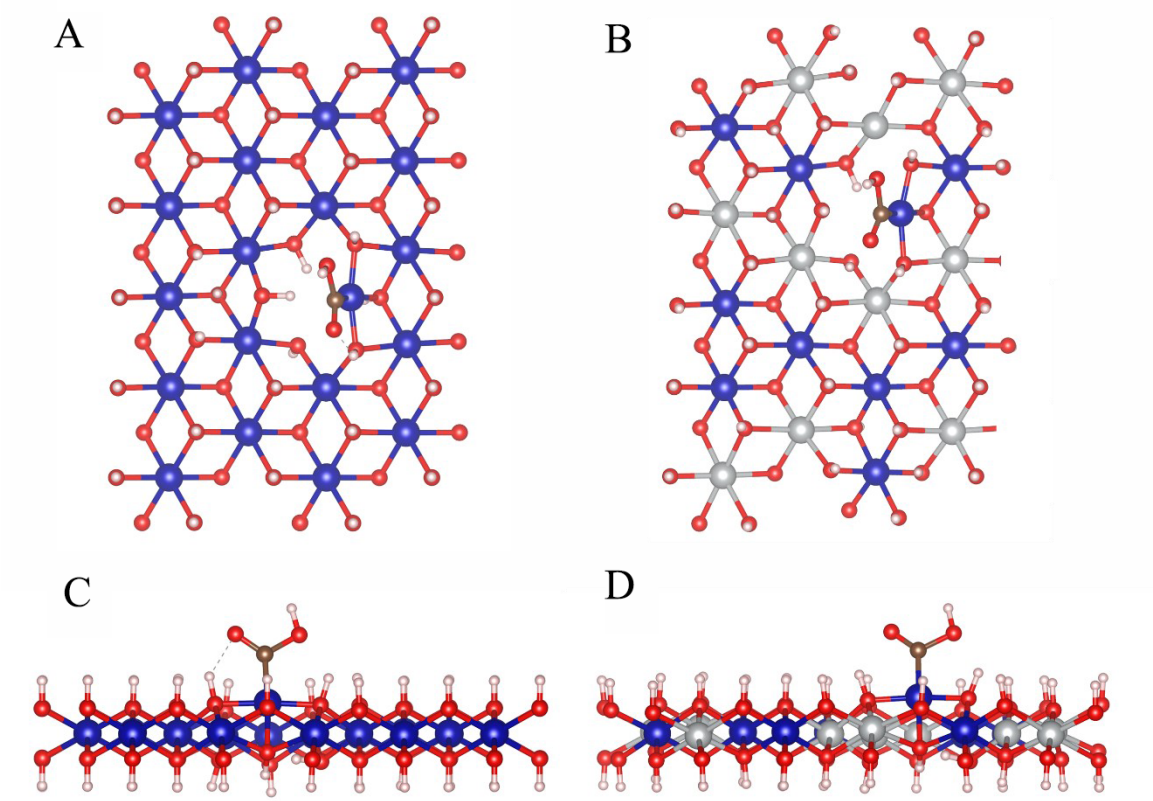

Fig. S17. The top view of optimized structures with COOH adsorbed over (A) Co-OH UNLS and (B) Ni Co-OH UNLS; The side view of optimized structures with COOH adsorbed over (C) Co-OH UNLS and (D) Ni Co-OH UNLS.

Table S1. Raw data of inductive coupled plasma emission mass spectrometry test.

Sample	Mass of catalyst (mg)	Metered volume (mL)	Concentration of Ni (mg L^{-1})	Concentration of Co (mg L^{-1})	Molar ratio of Ni : Co
NiCo-OH UNLS	5.0	200.0	6.8196	6.3898	1.07 : 1

Table S2. Visible-light-driven CO_2 reduction under various conditions.

Entry	Catalyst	Gas products ($mmol \cdot g^{-1} \cdot h^{-1}$)		CO selectivity (%) [a]
		CO	H_2	
1	NiCo-OH UNLS	309.5	30.6	91.0
2	Co-OH UNDH	192.1	153.1	55.7
3	NiCo-OH UNDH	170.8	20.4	89.3
4[b]	-	12.0	2.4	83.0
5[c]	NiCo-OH UNLS	0	0	-
6[d]	NiCo-OH UNLS	0	0	-
7[e]	NiCo-OH UNLS	0	0	-
8[f]	NiCo-OH UNLS	0	21.3	0

[a] The selectivity of CO was calculated by the equation of $n(CO)/[n(CO)+n(H_2)]*100\%$.

[b] Unit: $\mu mol \cdot h^{-1}$.

[c] Without TEOA.

[d] Without light.

[e] Without **Ru**.

[f] 1.0 atm Ar instead of 1.0 atm pure CO_2.

Table S3. Summary of photocatalytic CO_2 reduction activities of various photocatalytic systems.

Catalyst	Light source	Electron donor Photosensitizer	CO evolution ($mmol \cdot g^{-1} \cdot h^{-1}$)	CO selectivity (%)	Ref.
NiCo-OH UNLS	36 W 450 nm LED lamp	TEOA $[Ru(bpy)_3]Cl_2$	309.5	91.0	This work
Co-OH UNDH	36 W 450 nm LED lamp	TEOA $[Ru(bpy)_3]Cl_2$	192.1	55.7	This work
NiCo-OH UNDH	36 W 450 nm LED lamp	TEOA $[Ru(bpy)_3]Cl_2$	170.8	89.3	This work
$Cu_2S@R_{OH}$-$NiCo_2O_3$ DSNBs	300 W Xe lamp	TEOA $[Ru(bpy)_3]Cl_2$	7.1	72.0	[1]
$NC@NiCo_2O_4$	300 W Xe lamp	TEOA $[Ru(bpy)_3]Cl_2$	26.2	88.6	[2]
Ni-Co_3O_4 NSDHN	300 W Xe lamp	$Ru(bpy)_3Cl_2 \cdot 6H_2O$ TEOA	277.7	92.0	[3]
$Ni(OH)_2$-10%GR	300 W Xe lamp	$Ru(bpy)_3Cl_2 \cdot 6H_2O$ TEOA	10.7	96	[4]
ZnCo-OH QUNH	300 W Xe lamp	$Ru(bpy)_3Cl_2 \cdot 6H_2O$ TEOA	671.3	76.9	[5]
UiO-Co-N_3	300 W Xe lamp	$Ru(bpy)_3Cl_2 \cdot 6H_2O$ BIH	0.179	99.3	[6]
NiCoOP-NPs@MHCFs	300 W Xe lamp	$Ru(bpy)_3Cl_2 \cdot 6H_2O$ TEOA	166	65.9	[7]
$Ni(OH)_2$-NC-2	100 W 420 nm LED lamp	$Ru(bpy)_3Cl_2 \cdot 6H_2O$ TEOA	144	96.1	[8]

Reference

1. L. Li, X. Dai, D. Chen, Y. Zeng, Y. Hu and X. W. D. Lou, *Angew. Chem. Int. Ed.*, 2022, 61, e202205839.
2. S. Wang, B. Guan and X. Lou, *Energy Environ. Sc*i., 2018, 11, 306-310.
3. G. Qian, W. Lyu, X. Zhao, J. Zhou, R. Fang, F. Wang and Y. Li, *Angew. Chem. Int. Ed.*, 2022, 61, e202210576.
4. K. Lu, Y. Li, F. Zhang, M. Qi, X. Chen, Z. Tang, Y. M. A. Yamada, M. Anpo, M. Conte and Y. Xu, *Nat. Commun.*, 2020, 11, 5181.
5. F. Wang, R. Fang, X. Zhao, X. Kong, T. Hou, K. Shen and Y. Li, *ACS Nano*, 2022, 16, 4517-4527.
6. J. Wang, K. Sun, D. Wang, X. Niu, Z. Lin, S. Wang, W. Yang, J. Huang and H. Jiang, *ACS Catal.*, 2023, 13, 8760-8769.
7. Y. Wang, S. Wang and X. Lou, *Angew. Chem. Int. Ed.*, 2019, 58, 17236-17240.
8. Y. Su, Z. Song, W. Zhu, Q. Mu, X. Yuan, Y. Lian, H. Cheng, Z. Deng, M. Chen, W. Yin and Y. Peng, *ACS Catal.*, 2020, 11, 345-354.